PCT

INTERNATIONAL APPLICATION PUBLISHED UNDER THE PATENT COOPERATION TREATY (PCT)

(51) International Patent Classification 5 : A61B 5/0452	**A1**	(11) International Publication Number: **WO 94/06350**
		(43) International Publication Date: 31 March 1994 (31.03.94)

(21) International Application Number: PCT/US93/08782

(22) International Filing Date: 16 September 1993 (16.09.93)

(30) Priority data:
07/948,529   22 September 1992 (22.09.92)   US

(71) Applicant: GEORGETOWN UNIVERSITY [US/US]; 2nd Ryan Administration Building, 37th & O Streets, N.W., Washington, DC 20057 (US).

(72) Inventors: VERRIER, Richard, L. ; 5104 Duvall Drive, Bethesda, MD 20816 (US). NEARING, Bruce, D. ; P.O. Box 10434, Rockville, MD 20849 (US).

(74) Agents: KESSLER. Edward, J. et al.; Sterne, Kessler, Goldstein & Fox, 1100 New York Avenue, N.W., Suite 600, Washington. DC 20005-3934 (US).

(81) Designated States: AU, CA, JP, European patent (AT, BE, CH, DE, DK, ES, FR, GB, GR, IE, IT, LU, MC, NL, PT, SE).

Published
With international search report.
Before the expiration of the time limit for amending the claims and to be republished in the event of the receipt of amendments.

(54) Title: CARDIAC VULNERABILITY TRACKING METHOD AND APPARATUS

(57) Abstract

A method and apparatus for the non-invasive, dynamic tracking and diagnosing of cardiac vulnerability to ventricular fibrillation features simultaneous analysis of T-wave alternans (206) and heart rate variability (204). The T-wave alternation is an absolute predictor of cardiac electrical instability. Heart rate variability is a measure of autonomic influence, a major factor in triggering cardiac arrythmias By simultaneously analyzing both phenomena (208) the extent and cause of cardiac vulnerability can be assessed.

CARDIAC VULNERABILITY TRACKING METHOD AND APPARATUS

5   STATEMENT AS TO RIGHTS TO INVENTIONS MADE UNDER
    FEDERALLY SPONSORED RESEARCH AND DEVELOPMENT

Part of the work performed during development of this invention utilized U.S. Government funds. The U.S. Government has certain rights in this invention.

10 BACKGROUND OF THE INVENTION

1.   RELATED APPLICATION

This application is a continuation-in-part of application serial number 07/768,054, filed September 30, 1991, to issue as U.S. Pat. No. 5,148,812 on September 22, 1992; which is a continuation-in-part of application serial
15 number 07/659,711, filed February 20, 1991, now abandoned.

2.   FIELD OF THE INVENTION

The invention relates to cardiology. More specifically, the invention relates to non-invasive identification and management of individuals at risk for sudden cardiac death. Cardiac vulnerability to ventricular fibrillation, the
20 mode of sudden death, is dynamically tracked by analysis of an electrocardiogram.

3.   RELATED ART

Sudden cardiac death (SCD), which claims over 350,000 lives annually in the United States, results from abrupt disruption of heart rhythm primarily
25 due to ventricular fibrillation. Fibrillation occurs when transient neural triggers impinge upon an electrically unstable heart causing normally organized electrical activity to become disorganized and chaotic. Complete cardiac dysfunction results.

-2-

The first step in preventing sudden cardiac death is identifying those individuals whose hearts are electrically unstable. This is a major objective in cardiology. If vulnerable individuals can be reliably identified non-invasively, then prevention will be aided, mass screening will become

5   possible, and pharmacologic management of vulnerable individuals can be tailored to prevent ventricular fibrillation.

Programmed cardiac electrical stimulation has been used in patients to provide quantitative information on susceptibility and on the effectiveness of their pharmacologic therapy. Unfortunately, this method requires cardiac

10 catheterization and introduces the hazard of inadvertent induction of ventricular fibrillation. Therefore, it is used only in severely ill patients and is performed only in hospitals. It is unsuitable for mass screening.

A technique which has shown great promise is that of analyzing alternans in the T-wave of an electrocardiogram (ECG). As used throughout

15 this disclosure, the term "T-wave" is defined to mean the portion of an ECG which includes both the T-wave and the ST segment. Alternans in the T-wave results from different rates of re-polarization of the muscle cells of the ventricles. The extent to which these cells recover (or re-polarize) non-uniformly is the basis for electrical instability of the heart.

20 The consistent occurrence of alternans in the T-wave prior to fibrillation is well established. Thus, detection of alternans promises to be a useful tool in predicting vulnerability to fibrillation, if an accurate method of quantifying the alternans can be developed. The following are examples of conventional attempts to quantify alternation in an ECG signal: Dan R. Adam

25 et al., "Fluctuations in T-Wave Morphology and Susceptibility to Ventricular Fibrillation," *Journal of Electrocardiology*, Vol. 17 (3), 209-218 (1984); Joseph M. Smith et al. "Electrical Alternans and Cardiac Electrical Instability," *Circulation*, Vol. 77, No. 1, 110-121 (1988); U.S. Pat. No. 4,732,157 to Kaplan et al.; and U.S. Pat. No. 4,802,491 to Cohen et al.

30 Smith et al. and Cohen et al. disclose methods for assessing myocardial electrical instability by power spectrum analysis of the T-wave. These methods derive an alternating ECG morphology index from a series of

-3-

heartbeats. Sample point matrices are constructed and the alternating energy at each of the sample points is computed using the analytical method of multi-dimensional power spectral estimation which is calculated by constructing the discrete Fourier transform of the Hanning-windowed sample auto-correlation

5   function.   The alternating energy over the entire set of sample points is summed to generate the total alternating energy and then normalized with respect to the average waveform to produce an "alternating ECG morphology index (AEMI)."

While a powerful tool, Fourier power spectrum analysis averages time

10   functions over the entire time series so that rapid arrhythmogenic changes, such as those due to neural discharge and reperfusion, are not detected because data from these events are intrinsically non-stationary.

Kaplan et al. disclose a method for quantifying cycle-to-cycle variation of a physiologic waveform such as the ECG for the purpose of assessing

15   myocardial electrical stability.   A physiologic waveform is digitized and sampled and a scatter plot of the samples is created.   Non-linear transformation of the sample points determines a single parameter which attempts to quantify the degree of alternation in the sampled waveform and which is associated with the susceptibility of the physiologic waveform to enter

20   into an aperiodic or chaotic state. Kaplan et al. suggest that "measurement of [this parameter] may provide an index of ECG waveform variability which may provide an improved correlation with susceptibility to ventricular fibrillation than previously available indices." See col.3, lines 15-19. Whether ventricular fibrillation is a chaotic state, however, is still very much in debate.

25   See D.T. Kaplan and R. J. Cohen, "Searching for Chaos in Fibrillation," Ann. N.Y. Acad. Sci., Vol. 591, pp. 367-374, 1990.

Adam et al. disclose a non-invasive method which involves spectral analysis of the alternation from beat-to-beat morphology of the ECG complex. The alternation of T-wave energy from beat-to-beat was measured to generate

30   a T-wave alternation index (TWAI).   This technique is unable to detect alternation in waveform morphology which results in alternating wave shapes of equal energy.   In addition, the amount of alternation detected per this

-4-

method is dependent on the static portion of the wave shape. That is, the same amount of alternation superimposed on a different amplitude signal will result in different values for the T-wave alternation index such that this technique could completely obscure the presence of alternation in the original

5   waveform morphologies.

In the absence of an effective method for dynamically quantifying the magnitude of alternation, identification of alternans as a precursor of life-threatening arrhythmias and provision of a test for cardiac vulnerability have been unattainable. In addition, the conventional attempts to quantify alternans

10   have employed inferior methods of alternans (i.e., ECG) sensing. The ECG signals used for the Cohen *et al.* analysis were sensed via epicardial (i.e., heart surface) electrodes or via lateral limb, rostral-caudal, and dorsal-ventral leads. Smith *et al.* sensed via leads I, aVF, and V_{1-2}. Adam *et al.* utilized ECG lead I "because in this lead the ratio of the amplitude of the pacing

15   stimulus artifact to the amplitude of the QRS complex was usually smallest." See Adam *et al.* at 210. Lead I, however, provides only limited information regarding the electrophysiologic processes occurring in the heart.

There have been occasional reports in the human literature noting the presence of T-wave alternans in the precordial leads. However, there has

20   been no suggestion of a superior lead configuration from the body surface which permits measurement of alternans as a quantitative predictor of susceptibility to ventricular fibrillation and sudden death. For example, alternans have been observed in precordial leads V_4 and V_5 during a PCTA (Percutaneous Transluminal Coronary Angioplasty) procedure on a fifty year-

25   old man. M. Joyal *et al.*, "ST-Segment Alternans During Percutaneous Transluminal Coronary Angioplasty," *Am. J. Cardiol.*, vol. 54, pp. 915-916 (1984). Similarly, alternans were noted in precordial leads V_4 through V_6 on a forty-four year-old man during and following a treadmill exercise. N. Belic, *et al.*, "ECG Manifestations of Myocardial Ischemia," *Arch. Intern. Med.*,

30   vol. 140, pages 1162-1165 (1980).

Another method which has been explored to assess autonomic nervous system activity, the neural basis for vulnerability to sudden cardiac death is

-5-

analysis of heart rate variability (HRV). Heart rate variability, however, is not an absolute predictor of SCD because there are major, non-neural factors which contribute to sudden death. These include: coronary artery disease, heart failure, myopathies, drugs, caffeine, smoke, environmental factors, and

5   others. Accordingly, techniques which rely on heart rate variability to predict cardiac electrical stability are not reliable.

Further, conventional techniques for analyzing heart rate variability have relied on power spectrum analysis. See, for example, Glenn A. Myers *et al.*, "Power Spectral Analysis of Heart Rate Variability in Sudden Cardiac

10   Death: Comparison to Other Methods," *IEEE Transactions on Biomedical Engineering*, Vol. BME-33, No. 12, December 1986, pp. 1149-1156. As discussed above, however, power spectrum (Fourier) analysis averages time functions over an entire time series so that rapid arrhythmogenic changes are not detected.

15   Complex demodulation as a method for analyzing heart rate variability is discussed in Shin *et al.*, "Assessment of Autonomic Regulation of Heart Rate Variability by the Method of Complex Demodulation," *IEEE Transactions on Biomedical Engineering*, Vol. 36, No. 2, February 1989, which is incorporated herein by reference. Shin *et al.* teach a method of

20   evaluating the influence of autonomic nervous system activity during behavioral stress. A technique of complex demodulation is used to analyze the pattern of beat-to-beat intervals to determine the relative activity of the sympathetic and parasympathetic nervous systems. While Shin *et al.* exploited the dynamic analytical characteristics of complex demodulation, they did not

25   relate their results to cardiac vulnerability.

Similarly, T. Kiauta *et al.* "Complex demodulation of heart rate changes during orthostatic testing," *Proceedings Computers in Cardiology*, (Cat. No. 90CH3011-4), IEEE Computer Society Press, 1991, pp. 159-162, discusses the use of complex demodulation to assess heart rate variability

30   induced by the standing-up motion in young healthy subjects. Using the technique of complex demodulation, Kiauta *et al.* conclude that the complex demodulate of the high frequency band probably reflects parasympathetic

-6-

activity, but the complex demodulate of the low frequency band does not seem to indicate sympathetic activity. Similar to Shin *et al.*, Kiauta *et al.* do not relate their results to cardiac vulnerability.

In summary, analysis of the morphology of an ECG (i.e., T-wave
5   alternans) has been recognized as a means for assessing cardiac vulnerability. Similarly, analysis of heart rate variability has been proposed as a means for assessing autonomic nervous system activity, the neural basis for cardiac vulnerability. When researching vulnerability to sudden cardiac death, researchers have conventionally relied on power spectrum (Fourier) analysis.
10 However, power spectrum analysis is not capable of tracking many of the rapid arrhythmogenic changes which characterize T-wave alternans and heart rate variability. As a result, a non-invasive diagnostic method of predicting vulnerability to sudden cardiac death by analysis of an ECG has not achieved clinical use.

15   What is needed is a non-invasive, dynamic method for completely assessing vulnerability to ventricular fibrillation under diverse pathologic conditions relevant to the problem of sudden cardiac death. Among the most significant problems are enhanced discharge by the sympathetic nervous system, behavioral stress, acute myocardial ischemia, reperfusion, effects of
20 pharmacologic agents on the autonomic nervous system, and intrinsic cardiac effects of pharmacologic agents. To accommodate these conditions, the method must not assume stationarity of data and must be sensitive to slowly varying amplitude and phase over time. The diagnostic system must be sensitive to the fact that the area of injury to the heart can vary significantly,
25 that extrinsic as well as intrinsic influences affect the electrical stability of the heart, and that the electrophysiologic end point to be detected must be fundamentally linked to cardiac vulnerability.

-7-

SUMMARY OF THE INVENTION

The present invention is a method and apparatus for non-invasive, dynamic tracking and diagnosing of cardiac vulnerability to ventricular fibrillation. It is non-invasive as it detects vulnerability from leads placed on
5   the surface of the chest. Tracking and diagnosis of cardiac electrical stability are achieved through simultaneous assessment of both T-wave alternans and heart rate variability. The method permits tracking of transient but deadly pathophysiologic events, such as enhanced discharge by the sympathetic nervous system, behavioral stress, acute myocardial ischemia and reperfusion.
10   T-wave alternans and heart rate variability are simultaneously evaluated. T-wave alternation is an absolute predictor of cardiac electrical stability. Heart rate variability is a measure of autonomic influence, a major factor in triggering cardiac arrythmias. By simultaneously analyzing both phenomena, the extent and cause of cardiac vulnerability can be assessed.
15   This has important ramifications for tailoring and assessing the efficacy of drug therapy.

The method includes the following steps. A heart is monitored to sense an ECG signal. The sensed ECG signal is then amplified and low-pass filtered before it is digitally sampled and stored. Estimation of alternans amplitude
20   and analysis of heart rate variability are then separately performed.

Estimation of the amplitude of alternans is performed as follows. The location of the T-wave in each R-R interval (heart beat) of the ECG is estimated, and each T-wave is partitioned into a plurality of time divisions. The sampled ECG signal in each of the time divisions is summed together and
25   a time series is formed for each of the time divisions such that each time series includes corresponding time divisions from successive T-waves. The time series are detrended before further processing in order to remove the effects of drift and DC bias.

Dynamic estimation is performed on each time series to estimate the
30   amplitude of alternation for each time division. The preferred method of dynamic estimation is Complex Demodulation. Other methods include Estimation by Subtraction, Least Squares Estimation, Auto Regressive

-8-

Estimation, and Auto Regressive Moving Average Estimation. The amplitude of alternation is used as an indication of cardiac susceptibility to ventricular fibrillation (i.e., cardiac electrical instability).

Analysis of heart rate variability is performed as follows. The apex of
5   each R-wave is determined, and the time between successive R-waves is computed to determine a magnitude (time) of each R-R interval. The magnitude of each R-R interval is then compared to a predetermined criterion to eliminate premature beats. Next, a time series of the magnitudes of the R-R intervals is formed. Dynamic estimation is performed on the time series to
10 estimate the magnitude of a high frequency component of heart rate variability and to estimate the magnitude of a low frequency component of heart rate variability.

The magnitude of the high frequency component of heart rate variability is indicative of parasympathetic activity. The magnitude of the low
15 frequency component of heart rate variability is indicative of combined sympathetic activity and parasympathetic activity. A ratio of the low frequency component and the high frequency component of heart rate variability is formed. The ratio is indicative of sympathetic activity or vagal withdrawal.

20   In one embodiment of the invention, the ECG is sensed non-invasively via the precordial or chest leads. Leads V_5 and/or V_6 detect the optimal alternans signal when the left side (the most common site of injury for the propagation of life-threatening arrhythmias) of the heart is ischemic or injured. Leads V_1 and/or V_2 are optimal for detecting obstruction of the right-sided
25 coronary circulation. Additional precordial leads, such as V_9, may be useful for sensing alternans resulting from remote posterior wall injury. A physician may use the complete precordial lead system to obtain precise information non-invasively regarding the locus of ischemia or injury.

In alternate embodiments, the ECG is sensed via a catheter inserted
30 into the apex of either the left or right ventricles of the heart.

-9-

BRIEF DESCRIPTION OF THE DRAWINGS

FIG. 1A is a typical ECG plot.

FIG. 1B shows a number of heart rate plots with corresponding spectral plots.

FIG. 2A is high-level block diagram illustrating the diagnostic principles of the present invention.

FIG. 2B is a block diagram illustrating the diagnostic principles of the present invention in a first example.

FIG. 2C is high-level block diagram illustrating the diagnostic principles of the present invention in a second example.

FIG. 3 is a flow chart illustrating the method of the present invention.

FIG. 4 is a flow chart detailing the process of dynamically estimating the amplitude of T-wave alternans (as performed in step 314 of FIG. 3).

FIG. 5 is a flow chart detailing the process of dynamically analyzing heart rate variability to determine the activity of the autonomic nervous system (as performed in step 314 of FIG. 3).

FIG. 6A is a high-level block diagram of the apparatus of the invention.

FIG. 6B is a detailed block diagram of ECG detector and pre-processor 602.

FIG. 6C is a detailed block diagram of ECG processing system 604 comprising a microcomputer.

FIG. 7 is a detailed block diagram of the preferred embodiment of the heart monitoring unit (HMU) 600.

FIG. 8(a) is an ECG recorded within the left ventricle of a dog before coronary artery occlusion as set forth in the animal study below.

FIG. 8(b) shows superimposition of six successive beats from FIG. 8(a) presented on an expanded time scale.

FIG. 9(a) is an ECG recorded within the left ventricle of a dog after four minutes of coronary artery occlusion as set forth in the animal study below.

FIG. 9(b) shows superimposition of six successive beats from FIG. 9(a) presented on an expanded time scale.

FIG. 10(a) is an ECG recorded within the left ventricle of a dog after release of the coronary artery occlusion (during reperfusion) as set forth in the

5   animal study below.

FIG. 10(b) shows superimposition of six successive beats from FIG. 10(a) presented on an expanded time scale.

FIG. 11(a) is a surface plot of the T-wave of the ECG for eight dogs with intact cardiac innervation showing the effects of coronary artery occlusion

10   and reperfusion.

FIG. 11(b) is a surface plot of the T-wave of the ECG for six dogs after bilateral stellectomy showing the effects of coronary artery occlusion and reperfusion.

FIG. 11(c) is a surface plot of the T-wave of the ECG for eleven dogs

15   during thirty seconds of stimulation of the ansa subclavia of the decentralized left stellate ganglion showing the effects of coronary artery occlusion and reperfusion.

FIG. 12 shows the correlation between the occurrence of spontaneous ventricular fibrillation and T-wave alternans in ten dogs.

20   FIG. 13 is a graph showing the responses of the sympathetic and parasympathetic nervous systems to LAD coronary artery occlusion and reperfusion as indicated by heart rate variability.

FIGS. 14(a)-(c) illustrate the positioning of the precordial ECG leads on the body.

25   FIG. 15 is a cross-section of the human body illustrating the positioning of precordial ECG leads V_1-V_6 relative to the heart.

FIG. 16(a) is an ECG recorded from lead II during coronary artery occlusion in a dog.

FIG. 16(b) shows superimposition of six successive beats from FIG.

30   16(a) presented on an expanded time scale.

FIG. 17(a) is an ECG from precordial lead V_5 recorded simultaneously with the ECG of FIG. 16(a).

-11-

FIG. 17(b) shows superimposition of six successive beats from FIG. 17(a) presented on an expanded time scale.

FIG. 18(a) is an ECG from a left ventricular intracavitary electrode recorded simultaneously with the ECG of FIG. 16(a).

5   FIG. 18(b) shows superimposition of six successive beats from FIG. 18(a) presented on an expanded time scale.

FIG. 19 is a graph showing the relative magnitudes of alternans signals sensed from lead II and from precordial lead V_5 with reference to a left ventricular intracavitary electrode.

10   FIG. 20 is a surface plot display obtained by the method of complex demodulation (as set forth above) of the T-wave of the V_4 precordial lead during spontaneous heart rhythm in a representative patient during angioplasty.

FIG. 21 shows the level of T-wave alternans as a function of recording site in seven patients at three minutes of angioplasty-induced occlusion and 15   upon balloon deflation.

DETAILED DESCRIPTION OF THE PREFERRED EMBODIMENT
INTRODUCTION

Figure 1A shows a representative human surface ECG 100. A deflection 102 is known as the "P-wave" and is due to excitation of the atria. 20   Deflections 104, 106 and 108 are known as the "Q-wave," "R-wave," and "S-wave," respectively, and result from excitation (de-polarization) of the ventricles. Deflection 110 is known as the "T-wave" and is due to recovery (re-polarization) of the ventricles. One cycle (i.e., cardiac cycle or heart beat) of the ECG from the apex of a first R-wave to the apex of the next R-wave 25   is known as the R-R or interbeat interval. Heart rate variability (HRV) refers to changes in the heart rate (HR) or length (time) of the interbeat interval from one beat to the next.

A portion 112 between S-wave 108 and T-wave 110 of ECG 100 is known as the "ST segment". ST segment 112 includes the portion of the ECG 30   from the end of S-wave 108 to the beginning of the T-wave 110. Because this invention is concerned with alternans in the ST segment as well as in the T-

-12-

wave, the term "T-wave" in this disclosure, as noted above, includes both the
T-wave and the ST segment portions of the ECG.

The inventors have found that most alternans occurs in the first half of
the T-wave, the period of greatest vulnerability to ventricular fibrillation. See,
5 Nearing BD, Huang AH and Verrier RL, "Dynamic Tracking of Cardiac
Vulnerability by Complex Demodulation of the T Wave," *Science* 252:437-
440, 1991.

A more detailed discussion of ECG sensing and analysis is provided in
Dale Dubin, *Rapid Interpretation of EKG's*, 4th Edition, Cover Publishing
10 Company, 1990, which is expressly incorporated herein by reference.

Conventionally, autonomic nervous system activity, as indicated by
heart rate variability, has been researched as an independent indicator of
cardiac vulnerability (electrical stability). Autonomic nervous system activity,
however, is not an absolute predictor of cardiac vulnerability.

15 Further, conventional research has evaluated heart rate variability and
ECG morphology (as indicated by T-wave alternans) as independent variables
indicative of cardiac vulnerability. This also is an invalid assumption. HRV
and ECG morphology are linked, however, not invariably. Alternans can
change independently of HRV.

20 Heart rate variability and ECG morphology measure different aspects
of cardiovascular control. Both must be assessed in order to fully diagnose
cardiac vulnerability. The inventors have discovered that simultaneous
analysis of both heart rate variability and T-wave alternans yields important
diagnostic information pertaining to cardiac vulnerability. Heretofore, this
25 information has not been available.

By "simultaneous", it is meant that the analysis of T-wave alternans
and heart rate variability is carried out on the same ECG data. It is not
necessary for this to be done at the same time. For example, the ECG data
may be stored and the alternans analysis and heart rate variability analysis
30 performed in sequence one after the other.

Cardiac vulnerability is affected by both intrinsic and extrinsic factors.
The intrinsic factors include coronary artery occlusion and cardiomyopathy.

-13-

The extrinsic factors include the autonomic nervous system, pharmacologic agents, body chemistry (e.g., electrolytes), and other chemicals (e.g., from cigarette smoke, caffeine, etcetera).

An intrinsic factor can make a heart electrically unstable and therefore susceptible to SCD. T-wave alternans is indicative of cardiac electrical instability caused by intrinsic factors. Without T-wave alternans, a heart is not at risk of sudden cardiac death (ventricular fibrillation). As the magnitude of alternans increases, so does the risk of sudden cardiac death.

Extrinsic factors may also cause or increase the electrical instability of the heart by causing or increasing alternans. The autonomic nervous system is a primary extrinsic factor which affects cardiac electrical stability. Relative changes in actions of the parasympathetic system versus the sympathetic system can increase the magnitude of alternans, resulting in an increased vulnerability to SCD. However, a change in the autonomic nervous system by itself is not an absolute cause or predictor of cardiac electrical instability.

Heart rate variability is a measure of autonomic nervous system function. Generally, decreased heart rate variability will tend to increase the magnitude of alternans. Further, as described in detail below, analysis of the spectral content of heart rate variability indicates that the high frequency (e.g., 0.354 Hz) portion of the signal corresponds to parasympathetic (i.e., vagal) activity while the low frequency (e.g., 0.08 Hz) portion of the signal corresponds to combined sympathetic and parasympathetic activity.

A detailed discussion of heart rate modulation by the autonomic nervous system is provided in J. Philip Saul, "Beat-to-Beat Variations of Heart Rate Reflect Modulation of Cardiac Autonomic Outflow," *News in Physiological Sciences*, Vol. 5, February 1990, pp. 32-36.

Referring to Figure 1B (reproduced from *Id. at page 35*), Saul shows the heart rates and corresponding frequency spectra 120 for a patient with a normal heart, 122 for a patient with congestive heart failure, 124 for a diabetic patient with a peripheral neuropathy, 126 for a diabetic patient with a cardiac autonomic neuropathy, 128 for a patient with a transplanted heart prior to re-innervation, and 130 for a patient with a transplanted heart after re-

-14-

innervation. As can be seen from inspection of these data plots, the loss of neural activity either due to diabetes or cardiac transplant is evident in the absence of normal spectra. With return of normal innervation, the spectra at least partially return.

5   Figure 2A is a block diagram illustrating the diagnostic principles of the present invention. Block 202 represents all factors which affect the electrical function of the heart (e.g., drugs and/or diseases). Block 204 represents increased heart rate variability resulting from the factors of block 202. Block 206 represents alternation of the amplitude of the T-wave resulting
10   from the factors of block 202. Block 208 represents sudden cardiac death resulting from ventricular fibrillation.

As shown, the factors of block 202 can lead to SCD in block 208 by two major pathways. The first pathway is from block 202, through block 206, to block 208. This results from a direct influence of the factors of block 202
15   on the electrical stability of the heart, manifest in the form of T-wave alternans. This mode of SCD would occur without a change in heart rate variability because the nervous system is not involved. A corollary to this is that a sudden death prediction method which relies solely on heart rate variability would not be adequate to detect SCD.

20   The second major pathway from the factors of block 202 to SCD in block 208 is through blocks 204 and 206. This results from an influence of the factors of block 202 on the autonomic nervous system. Drugs or heart disease, for example, can significantly alter neural activity. This will be expressed as changed heart rate variability. Certain changes in neural activity
25   which increase sympathetic tone significantly increase T-wave alternans and therefore could result in SCD.

The inventors have discovered that by combining T-wave alternans measure and heart rate variability, it is possible, not only to assess risk for SCD accurately, but also to determine whether a derangement in autonomic
30   nervous system activity is causal. This has important clinical significance as it affects both diagnosis and therapy.

-15-

For example, terfenadine (Seldane) is a drug widely employed for the treatment of sinus problems. It has recently been discovered that, when terfenadine is used in conjunction with antibiotics, SCD can result. Terfenadine has no known effects on the autonomic nervous system and consequently does not affect heart rate variability. However, the drug can result in alternans in isolated heart preparations and is thus capable of directly de-stabilizing the electrical activity of the heart. The measurement of T-wave alternans is therefore an essential approach to detect susceptibility to SCD induced by a terfenadine/antibiotic combination. This is illustrated in Figure 2B.

For another example, digitalis drugs are the most commonly used agent for increasing the strength of contraction of diseased hearts. The drugs produce this effect by both direct influence on the heart and through alterations in the autonomic nervous system. In the proper therapeutic range, there is no significant negative effect on the electrical stability of the heart. However, when the dose is either too high or the patient's health status changes due to illness, the same dose of drug may become toxic. It is often difficult to determine whether a patient is under-dosed or overdosed. By using a combined alternans/HRV analysis, it would be possible to determine at what point a neurotoxic influence may lead to alternans and SCD. In particular, high doses of digitalis decrease vagal tone and increase sympathetic activity, effects which would be clearly detected in an heart rate variability analysis. This is illustrated in Figure 2C. This information would be a valuable asset in the therapeutic management of the patient.

As discussed above, traditional methods of quantifying heart rate variability or the magnitude of alternans have relied on power spectrum (Fourier) analysis. However, power spectrum analysis is not capable of tracking many of the rapid arrhythmogenic changes which characterize T-wave alternans and heart rate variability. In the preferred embodiment, the present invention utilizes complex demodulation to analyze heart rate variability and T-wave alternans.

-16-

METHOD OF THE INVENTION

The method of the present invention for analyzing an ECG is now discussed with reference to Figures 3-5.

An ECG signal containing a plurality N of R-R intervals is sensed from
5   a patient in real time at step 302. The preferred method of non-invasively sensing the ECG signal is discussed in detail below. Because the body is akin to a dipole, a large DC component will be present in the sensed ECG. This DC component is removed at step 304 with a high-pass filter prior to amplification of the ECG signal at step 306. The amplified ECG signal is then
10   low-pass filtered at step 308 to limit the signal bandwidth before it is digitally sampled at step 310. The digitized data may then be stored on a magnetic or optical storage device at step 312. Finally, the digitized ECG data is dynamically processed at step 314 to: (1) produce an estimation of alternans amplitude and (2) estimate the magnitude of discrete spectral components of
15   heart rate variability to determine the sympathetic and parasympathetic influences on cardiac electrical stability.

As an alternative to this real-time signal pre-processing, the ECG signal may be retrieved from the storage device (step 312) and processed (step 314) at a later, more convenient time.

20   Processing step 314 involves two independent computations: alternans processing and heart rate variability processing. Each is discussed in detail below.

T-WAVE ALTERNANS

The analysis of alternans at step 314 is described in detail with
25   reference to Figure 4. At step 404, the apex of each R-wave in the signal data for each of the N beats is located by finding the peak amplitudes in the digitized signal. Premature beats are removed at step 406 by comparison of each R-R interval with fixed criteria. At step 408, a portion of the ECG corresponding to an estimated location (with respect to R-wave 106) of T-wave
30   110 is identified.

-17-

At step 410, the T-wave 110 and 112 portion of the ECG signal is partitioned into "B" time divisions, where "B" may include a single digital sample or a plurality of samples. The area between the ECG and the isoelectric baseline is computed for each time division, at step 412, by

5   summing the areas of all samples in the time division. Then at step 414, "N" successive beats (e.g., from control through release in the animal experiments discussed below) are sequenced into a time series for each of the "B" time divisions: $(X(n), n = 1,2,...N)$.

A high-pass filter is used for detrending the time series at step 416 to

10   remove the effects of drift and DC bias (e.g., high-pass filtering removes the large low-frequency variation in T-wave area that occurs during occlusion of a coronary artery). A cleaner signal is then available for dynamic estimation, which is performed at step 418 to estimate the amplitude of alternation for each time series.

15   The estimation of step 418 may be performed via several dynamic methods. By "dynamic" method, it is meant any analytical process sufficiently rapid to track (i.e., estimate) transient changes such as those which occur in alternans amplitude in response to physiologic and pathophysiologic processes triggering arrhythmias. These include, for example, enhanced neural

20   discharge, acute myocardial ischemia and reperfusion. A "dynamic" method should be able to track alternans from as few as approximately ten heart beats (or less). This precludes analytic processes (e.g., Fourier power spectrum analysis) which require stationarity of data for several minutes. Specific, but not exclusive, examples of methods for dynamic estimation include:

25   (a)   Complex Demodulation,
         (b)   Estimation by Subtraction,
         (c)   Least Squares Estimation,
         (d)   Auto-Regressive (AR) Estimation, and
         (e)   Auto-Regressive Moving Average (ARMA) Estimation.

-18-

(A)   COMPLEX DEMODULATION

Complex demodulation is the preferred method of dynamic estimation of the beat-to-beat alternation in the amplitude of each time series. Complex demodulation is a type of harmonic analysis which provides a continuous

5   measure of the amplitude and phase of an oscillation with slowly changing amplitude and phase. It detects features that might be missed or misrepresented by standard Fourier spectral analysis methods which assume stationarity of data.

By definition, alternans is a periodic alternation in the T-wave. The

10   magnitude of alternans, however, changes slowly during a coronary artery occlusion and more rapidly during release, making it quasi-periodic. As such, it must be represented by a sinusoid with slowly varying amplitude, $A(n)$, and phase, $\phi(n)$:

$$X(n) = A(n) \cos[2\pi f_{ALT} + \phi(n)] \qquad \text{Eq. (1)}$$

15   where: $X(n) =$ the data sequence with alternation in its amplitude

                $f_{ALT} =$ alternation frequency (Hz). It should be noted that this frequency is half of the heart rate.

Using the identity

$$\cos(x) = \frac{e^{jx} + e^{-jx}}{2}, \qquad \text{Eq. (2)}$$

the equation for $X(n)$ can be rewritten as

$$X(n) = A(n) \times \frac{(e^{j2\pi f_{ALT} n} \, e^{j\phi n} + e^{-j2\pi f_{ALT} n} \, e^{-j\phi n})}{2} \qquad \text{Eq. (3)}$$

20   The method of complex demodulation requires multiplying this time series $X(n)$ by two times a complex exponential at the alternans frequency [to produce $Y_1(n)$] and then filtering the result to retain only the low frequency term $Y_2(n)$ as follows:

-19-

$$Y_1(n) = X(n) \times 2e^{-j2\pi f_{ALT} n}$$
$$= A(n) \, [e^{j\phi(n)} + e^{-j4\pi f_{ALT} n - j\phi(n)}]$$ Eq. (4)

$$Y_2(n) = A(n) \, e^{j\phi(n)}$$ Eq. (5)

The amplitude and phase of the alternans is then found from the filtered signal, $Y_2(n)$, as follows:

$$A(n) = |Y_2(n)|$$
$$= magnitude \ of \ Y_2(n)$$ Eq. (6)
$$= \sqrt{Re[Y_2(n)]^2 + Im[Y_2(n)]^2}$$

$$\phi(n) = phase \ of \ Y_2(n)$$
$$= \arctan\left[\frac{Im[Y_2(n)]}{Re[Y_2(n)]}\right]$$ Eq. (7)

where: Im and Re refer to the imaginary and real parts of Y_2

For a more detailed discussion of complex demodulation, see *Fourier*
5   *Analysis of Time Series: An Introduction*, by Peter Bloomfield, John Wiley &
Sons: New York, pp. 118-150; which is incorporated herein by reference.

(B)   ESTIMATION BY SUBTRACTION

The subtraction method of dynamic estimation is an alternative which
may be substituted for complex demodulation. The subtraction method
10   involves subtracting the area of each time division (n) of an R-to-R interval
from the area of the corresponding time division of a subsequent (n + 1), or
alternatively, a previous (n-1) R-to-R interval to form a new time series Y(n)
representing the magnitude of alternans. Because this difference series Y(n)
may be positive or negative, the absolute value or magnitude of Y(n) is used
15   for the magnitude A(n). That is:

$$Y(n) = X(n) - X(n-1)$$ Eq. (8)

-20-

$$A(n) = |Y(n)|$$
$$= |X(n) - X(n-1)|$$
$$= \text{magnitude of alternans} \qquad \text{Eq. (9)}$$

Some errors may be introduced into this estimate due to the slowly varying increase in magnitude of the T-wave size at the start of a coronary occlusion and the reduction in size following the occlusion. Also, some T-wave variation due to respiration is expected. Therefore detrending the
5   sequence X(n) using a high pass digital filter, or equivalent, improves the estimate by removing the effects of T-wave size changes. Also, averaging M samples together, where M is the number of beats occurring during a single respiratory cycle, aids in eliminating the respiratory effects on the estimate. Alternatively, the digital filter may remove both trends and respiratory changes
10   if the respiration frequency is sufficiently different from the heart rate, so that the filtering does not alter the magnitude of the alternans estimate.

(C)   LEAST SQUARES ESTIMATION

The least squares estimation, which also turns out, in this case, to be the maximum likelihood estimate for estimating sinusoid amplitude in white
15   noise, is a second alternative which may be substituted for complex demodulation to calculate a new sequence which is a dynamic estimate of the amplitude of alternans. Least squares estimation of the amplitude of alternans A(n) for the data sequence X(n) is derived as follows.

Assume for M points (e.g., 5 to 10 cardiac cycles) that:

$$X(n) = A \cos(2\pi f_{ALT} n) + N(n) \qquad \text{Eq. (10)}$$

20   where: N(n) represents additive noise

In order to minimize the noise term and estimate the alternans component, create a new function T(A), where:

$$T(A) = \sum_{j=n}^{n+M-1} [X(j) - A \cos(2\pi f_{ALT} j)]^2 \qquad \text{Eq. (11)}$$

-21-

T(A) represents a measure of the difference between the model and the data. The best alternans magnitude estimate results if T(A) (i.e., the noise term) is minimized. To minimize T(A), take the derivative of T(A) with respect to A and set it equal to zero:

Eq. (12)

$$\frac{\delta T}{\delta A} = -2 \times \sum_{j=n}^{n+M-1} \{\cos(2\pi f_{ALT}j) \ [X(j) - A \ \cos(2\pi f_{ALT}j)]\} = 0$$

5   Next, solve this equation for A(n) (shown simply as "A" above) and take the absolute value of the result to yield the least squares estimate of the magnitude of the alternans:

Eq. (13)

$$A(n) = \frac{1}{M} \left| \sum_{j=n}^{n+M-1} [X(j) \ \cos(2\pi f_{ALT}j)] \right|$$

(D)   AUTO-REGRESSIVE ESTIMATION (AR)

Auto-Regressive (AR) Estimation is a third method of dynamic
10   estimation which may be substituted for complex demodulation.   AR estimation models the alternans as follows:

Eq. (14)

$$X(n) = - \sum_{k=1}^{P} [a(k) \times X(n - k)] + u(n)$$

In this model, "P" is the number of auto regressive coefficients chosen for the estimation.   u(n) represents noise and accounts for the imperfect fit of the estimation. The method of estimating the amplitude of alternans A(n) for the

-22-

data sequence X(n) first involves calculating a matrix of co-variance coefficients c(i,k) according to the following formula:

Eq. (15)

$$c(i,k) = \frac{1}{M-P} \sum_{j=n+P}^{n+M-1} [X(j - i) \times X(j - k)]$$

where: â = the best estimate of the true value of "a"
P = the number of auto regressive coefficients "â"
M = the number of cardiac cycles

The co-variance coefficients are then used to form "P" auto regressive coefficients "â" as follows:

Eq. (16)

$$\begin{vmatrix} \hat{a}(1) \\ \hat{a}(2) \\ \vdots \\ \hat{a}(P) \end{vmatrix} = - \begin{vmatrix} c(1,1) & c(1,2) & \cdots & c(1,P) \\ c(2,1) & c(2,2) & \cdots & c(2,P) \\ \vdots & & & \\ c(P,1) & c(P,2) & \cdots & c(P,P) \end{vmatrix}^{-1} \times \begin{vmatrix} c(1,0) \\ c(2,0) \\ \vdots \\ c(P,0) \end{vmatrix}$$

The estimate of the alternans magnitude is then given by:

Eq. (17)

$$A(n) = \frac{\sigma^2}{1 - \sum_{n=1}^{P} \hat{a}(n) e^{-j2\pi f_{ALT} T^n}}$$

$$where: \quad \sigma^2 = c(0,0) + \sum_{n=1}^{P} \hat{a}(n) c(0,n)$$

For a more detailed discussion of auto-regressive estimation, see *Modern Spectral Estimation: Theory and Applications*, by Steven Kay, Prentice Hall, 1988, pp. 222-225; incorporated herein by reference.

(E)   AUTO-REGRESSIVE MOVING AVERAGE (ARMA) ESTIMATION

Auto-Regressive Moving Average (ARMA) Estimation is yet another dynamic method which may be substituted for complex demodulation. ARMA

-23-

estimation involves modeling the alternans with a data sequence X(n) as follows:

Eq. (18)

$$X(n) = -\sum_{k=1}^{P} [a(k) \times X(n - k)] + \sum_{k=0}^{q} [b(k) \times u(n - k)]$$

Note that this equation is similar to the model of X(n) according to the AR method, however, additional coefficients "b(k)" have been added to the model.

5   These coefficients are necessary when the spectrum of the data has contours which are more complex than just spikes due to alternans and respiration periodicities. Let "â" and "b̂" be the best estimates of "a" and "b". The auto regressive coefficient estimates are found by performing Newton Raphson Iteration to find the zeros of:

Eq. (19)

$$\left[\left(\frac{\delta Q}{\delta a} \right)^T \times \left(\frac{\delta Q}{\delta b} \right)^T \right]^T$$

10   This minimizes the error function:

Eq. (20)

$$Q(a,b) = \int_{-1/2}^{1/2} I(f) \frac{|A(f)|^2}{|B(f)|^2} \, df$$

$$\text{where:} \quad I(f) = \frac{1}{M} \left| \sum_{n=0}^{M-1} X(n) \, e^{-j2\pi f n} \right|^2$$

$$A(f) = 1 - \sum_{k=1}^{q} a(k) e^{-j2\pi f k}$$

$$B(f) = \sum_{k=0}^{P} b(k) e^{-j2\pi f k}$$

-24-

The estimate of the alternans magnitude is then given by:

Eq. (21)

$$A(n) = \frac{\sigma^2 \sum_{k=1}^{q} \hat{b}(k) \, e^{-j2\pi f_{ALT}k}}{1 - \sum_{k=1}^{P} \hat{a}(k) \, e^{-j2\pi f_{ALT}k}}$$

$$\text{where:} \quad \sigma^2 = Q(\hat{a},\hat{b})$$

For a more detailed discussion of auto-regressive moving average estimation, see *Modern Spectral Estimation: Theory and Applications*, by Steven Kay, Prentice Hall, 1988, pp. 309-312; incorporated herein by reference.

The resultant time series A(n), representative of the magnitude of alternans, which is produced in step 418 (by one of the dynamic methods set forth above), may then be analyzed for diagnostic purposes. This may include producing a surface plot as shown in Figures 11(a)-(c) (described below).

It will be understood by one skilled in the art that the various steps of filtering set forth above may be performed by analog or digital means as discussed below. It will further be understood that each of the various filtering steps may be modified or eliminated from the method, if desired. Note, however, that detrending is particularly important for the Least Squares Estimate Method.

Elimination of the various filtering steps will, of course, lead to a reduction in clarity and will add corruption to the sought after signals. The amount of corruption will depend on the amount of noise present in the specific data. The noise sources sought to be filtered include: white noise, respiration induced electrical activity, premature beats, slowly varying trends present in the area under the ECG waveforms, and other miscellaneous noises.

-25-

HEART RATE VARIABILITY

The analysis of heart rate variability at step 314 is described in detail
with reference to Figure 5. At step 504, the apex of each R-wave in the
signal data for each of the N beats is located by finding the peak amplitudes
5   in the digitized signal. At step 506, the R-R intervals (time) between
successive R-waves is computed. Premature beats are then removed at step
508 by comparing each R-R interval with fixed criteria.

At step 510, a time series of R-R interval data is formed by listing the
R-R interval times in order. At step 512, a second time series or sequence
10   (R_t), whose points are 100 msec apart and whose values are the R-R intervals
present at that time, is formed along the same time line. For example, if the
R-R interval data for a certain ECG signal has the values:

300 msec, 350 msec, 400 msec . . . .,

then the series (R_t, t) would become:

15   (300,0), (300,100), (300,200), (350,300), (350,400), (350,500),
            (350,600), (400,700), (400,800), (400,900), (400,1000) . . . .

At step 514, the sequence (R_t) is filtered to remove any low frequency
trends. A cleaner signal is then available for dynamic estimation, which is
performed at steps 516 and 522 to estimate the magnitude of discrete spectral
20   components of heart rate to determine the sympathetic and parasympathetic
influences on cardiac electrical stability. This dynamic estimation at steps 516
and 522 is performed using similar methods (except for Estimation by
Subtraction) to those discussed above with respect to analysis of alternans at
step 418.

25   Specifically, the estimation at steps 516 and 522 may be performed via
Complex Demodulation, Auto-Regressive (AR) Estimation, Auto-Regressive
Moving Average (ARMA) Estimation, or other time domain methods.
Traditional power spectrum (Fourier) analysis may be used, however, it is not
recommended because it will produce inferior results and some data (e.g.,
30   rapid changes in heart rate) may be lost.

Complex demodulation is the preferred method of demodulating heart
rate variability. Complex demodulation of heart rate variability is performed

-26-

as follows. At step 516, the sequence (R_t) (from step 514) is multiplied by 2 $\cdot e^{(-j2\pi fn)}$, at f $\approx$ 0.10 Hz to yield the low frequency component of heart rate variability. "n" is the index of the data point in sequence (R_t). In parallel with the computation of the low frequency component of heart rate variability

5   at step 516, the high frequency component of heart rate variability is computed at step 522 by multiplying the sequence (R_t) by 2 $\cdot e^{(-j2\pi fn)}$, at f $\approx$ 0.35 Hz (i.e., a frequency close to the respiration frequency). The low frequency component of heart rate variability is then low pass filtered (e.g., roll-off frequency $\approx$ 0.10 Hz) at step 518. The high frequency component of heart

10   rate variability is low pass filtered (e.g., roll-off frequency $\approx$ 0.15 Hz) at step 524. It should be noted that low pass filtering (steps 518 and 524) is part of the method of complex demodulation (steps 516 and 522).

The magnitude of the high frequency (e.g., $\approx$ 0.35 Hz) component of heart rate is indicative of parasympathetic activity. The magnitude of the low

15   frequency (e.g., $\approx$ 0.10 Hz) component of heart rate, however, is affected by both sympathetic and parasympathetic activity. Therefore, to discern the influence of the sympathetic nervous system, the low frequency (LF) component of heart rate (from step 518) is divided by the high frequency (HF) component of heart rate (from step 524) at a step 520 to produce a ratio

20   (LF/HF). This ratio is indicative of the ratio of sympathetic activity to parasympathetic activity and can thus be used to assess sympathetic activity. Ratioing low and high frequency components of heart rate to estimate sympathetic activity is further described in M. Pagani, *et al.*, "Power Spectral Analysis of Heart Rate and Arterial Pressure Variabilities as a Marker of

25   Sympatho-Vagal Interaction in Man and Conscious Dog," *Circulation Research*, Vol. 59, No. 2, August 1986, pp. 178-193, incorporated herein by reference.

Steps 516,518 and 522,524 of the method described above detect heart rate variability using the method of complex demodulation. Analysis of heart

30   rate variability using the method of complex demodulation is further described in Shin *et al.*, discussed above.

-27-

APPARATUS OF THE INVENTION

       The preferred embodiment of the apparatus of the invention is described with reference to Figures 6 and 7. Steps 304-308 of the method may be performed using a conventional ECG machine or may be performed

5   using dedicated hardware. Similarly, steps 312 and 314 may be performed on a general purpose computer or may performed by dedicated hardware.

       In the preferred embodiment, the invention is carried out on a heart monitoring unit (HMU) 600, shown in Figure 6A. HMU 600 includes ECG sensing leads 601, an ECG detector and pre-processor 602 and an ECG

10   processing system 604. ECG detector and pre-processor 602, shown in greater detail in Figure 6B, includes a high-pass filter 6022, a pre-amplifier 6024, and a low-pass filter 6026. ECG sensing leads (i.e., electrodes) 601 provide a signal from a patient directly to high-pass filter 6022.

       In an alternate embodiment, ECG detector and pre-processor 602 is a

15   conventional ECG monitoring machine.

       Referring now to Figure 6C, ECG processing system 604 is described. ECG processing system 604 includes a programmed microcomputer 6040 equipped with an analog-to-digital (A/D) conversion board 6050. The steps of the method are performed using a software program written in C

20   Programming language. The program follows the steps set forth above. It is believed that any skilled programmer would have no difficulty writing the code necessary to perform the steps of this invention.

       Microcomputer or computer platform 6040 includes a hardware unit 6041 which includes a central processing unit (CPU) 6042, a random access

25   memory (RAM) 6043, and an input/output interface 6044. RAM 6043 is also called a main memory. Computer platform 6040 also typically includes an operating system 6045. In addition, a data storage device 6046 may be included. Storage device 6046 may include an optical disk or a magnetic tape drive or disk.

30   Various peripheral components may be connected to computer platform 6040, such as a terminal 6047, a keyboard 6048, and a printer 6049. Analog-to-digital (A/D) converter 6050 is used to sample an ECG signal. A/D

-28-

converter 6050 may also provide amplification of the ECG signal prior to sampling.

Figure 7 shows the preferred embodiment of HMU 600. The system includes 16 channels to allow simultaneous monitoring of a plurality of ECG

5   leads. High-pass filters 704, pre-amplifiers 706, and low-pass filters 708 perform steps 304, 306 and 308, respectively. High-pass filters 704 have a 0.01 Hz roll-on. Low-pass filters 708 have a 50 Hz bandwidth.

A personal computer 710 includes an A/D converter (with programmable gain), a printer 714, a re-writable optical disk 716, and a color

10   monitor 718. The program which runs on computer 710 is preferably menu-driven. A sample menu is shown on monitor 718.

The menu-driven program may take, as input, information on a patient's age, sex, medical history, and heart rate. This information could then be used to select a range of standard indices (discussed below) to be used

15   for comparison. The menu program would further allow the clinician/operator to select the A/D sampling rate, the number of ECG channels to monitor, and the gain of the A/D converter prior to commencing data collection. Thereafter, the clinician/operator could manually control removal of trends and premature beats prior to performing the dynamic analysis of alternans and

20   heart rate variability.

Features of the menu-driven program may include selecting the method of dynamic analysis to be used and selecting the results to be displayed. For example, the clinician/operator may desire to view the ECG waveforms, the time series data (e.g., for each bin of the T-wave both before and after

25   detrending for the alternans analysis; or for the R-R intervals in the HRV analysis), or the actual estimate data (e.g., alternans magnitude, HRV high frequency component, HRV low/high frequency component ratio).

-29-

ANIMAL STUDY FOR ALTERNANS ANALYSIS

Animal studies were conducted by the inventors at Georgetown University School of Medicine in Washington, D.C. Sixteen adult mongrel dogs (20 to 30 kg) of both sexes were studied in accordance with the standards
5   of the scientific community. The animals were pre-medicated with morphine sulfate (2 mg/kg, subcutaneously) and anesthetized with alpha-chloralose (150 mg/kg, intravenously), with supplemental doses of alpha-chloralose (600 mg in 60 ml saline) as required. A left thoracotomy was performed via the fourth intercostal space.

10   A Doppler flow probe was placed around the left anterior descending (LAD) coronary artery and occlusions were performed using a 2-0 silk snare. Aortic blood pressure was measured with a Gould-Statham P50 pressure transducer. The ECG was obtained using a 7 French USCI quadripolar catheter with an inter-electrode distance of 10 mm and an electrode width of
15   2 mm. The catheter was positioned in the apex of the left ventricle via a carotid artery to coincide with the ischemia. This catheter placement was found to produce optimal ECG sensing.

Bipolar ECG's were obtained with the negative pole being the second electrode of the catheter and the positive pole being a needle-electrode placed
20   transcutaneously in the lower left hip region. A pigtail pressure catheter was positioned to monitor left ventricular (LV) blood pressure. The area under the LV pressure pulse of successive beats was analyzed using the technique of complex demodulation. No evidence of mechanical alternans was found. The electrocardiographic and hemodynamic data were continuously recorded on a
25   Thorn EMI FM tape recorder (45 to 50 db S/N ratio, bandwidth of each channel 0 to 625 Hz). Arterial blood pH, pCO_2, and pO_2 were monitored using an Instrumentation Laboratory 1304 blood gas analyzer and were maintained within physiologic ranges by adjusting ventilation parameters of the Harvard respirator.

30   A bilateral stellectomy was performed to interrupt sympathetic neural input to the heart. This was accomplished by removal of the right stellate ganglion via the right second interspace and by sectioning the preganglionic

-30-

fibers and the caudal end of the left ganglion through the left thoracotomy.
The ansae subclavia were left intact to permit pacing of the heart at a rate of
150 beats per minute. Pacing was accomplished by delivering electrical
stimuli of 1.5 to 2 mA of 5 ms duration at a frequency of 10Hz to the nerves
5   with a Grass S44 stimulator and an SIU7 stimulus isolation unit.

At the end of each experiment, the taped data was low-pass filtered to
limit the signal bandwidth to 50 Hz. The data was then digitized at 500
samples per second, with a Compaq 386 computer equipped with a Metrabyte
DAS-20 A/D conversion board, and stored on an optical disk. The apex of
10   each R-wave for each of the N beats was then located by finding the peak
amplitudes in the digitized signal. Each beat was indexed by n from 1 to N.
The R-R interval was employed to sort out and remove premature beats which
could introduce artifactual spikes. The period from 60 to 290 ms following
the apex of each R-wave was determined to coincide with the location of the
15   T-wave. This period was divided into bins 10 ms wide for each successive
beat, and the area between the ECG and the isoelectric baseline was computed
for each 10 ms interval. N successive beats from control through release were
then sequenced into a time series for each of the 23 10-ms bins: $(X(n), n =
1,2,...N)$. A sixteenth order Butterworth filter was used for both detrending
20   and demodulating to remove the large low-frequency variation in T-wave area
that occurs during occlusion and to leave a cleaner signal for spectral
estimation.

Detrending was performed by low-pass filtering each time series with
the Butterworth filter and then subtracting the result from the original time
25   series to achieve a high-pass filtering function. To obtain estimates of the
magnitude of beat-to-beat alternation in the amplitude of each of these twenty-
three time series, complex demodulation (as set forth above) was used.

The effects of LAD coronary artery occlusion and reperfusion on T-
wave alternans were tested before and after sympathetic denervation and
30   stimulation. Baseline data was obtained for four minutes, the artery was
occluded for eight minutes followed by abrupt release (reperfusion) and a 30-

-31-

minute rest period. As set forth above, heart rate was maintained constant by
atrial pacing at 150 bpm during assessment of the magnitude of alternans.

In eight dogs, a preconditioning occlusion was followed by a control
occlusion with nerves intact. The occlusion-release sequence was repeated

5   after stellate ganglion ablation. Finally, the left stellate ganglion was
stimulated two to three minutes prior to occlusion, during the second and fifth
minutes of occlusion, and during reperfusion. In the second group of eight
dogs, the order of interventions was changed to rule out sequence-related error
by omitting the occlusion with nerves intact.

10   Figures 8(a)-10(a) show, respectively, an electrocardiogram recorded
within the left ventricle before, during, and after coronary artery occlusion in
a single representative animal. Figures 8(b)-10(b) show superimposition of six
successive beats. Prior to occlusion (Figure 8), the T-waves of each
succeeding beat are uniform. After four minutes of coronary artery occlusion

15   (Figure 9), there is marked alternation of the first half of the T-wave,
coinciding with the vulnerable period of the cardiac cycle. The second half
of the T-wave remains uniform. After release of the occlusion (Figure 10),
alternans is bidirectional, with T-waves alternately inscribed above and below
the isoelectric line.

20   Coronary artery occlusion and reperfusion both resulted in significant
increases in the magnitude of beat-to-beat alternation in T-wave amplitude.
Figure 11 shows a surface plot display derived by complex demodulation of
the T-wave of the electrocardiogram before, during, and after coronary artery
occlusion in eight dogs with intact cardiac innervation (Figure 11(a)); after

25   bilateral stellectomy in six dogs (Figure 11(b)); and during 30 sec of
stimulation of the ansa subclavia of the decentralized left stellate ganglion in
eleven dogs (Figure 11(c)).

The increase in alternans was evident within two to three minutes of
occlusion and progressed until the occlusion was terminated at eight minutes.

30   Upon reperfusion, there was an abrupt increase in alternans which lasted less
than one minute. A remarkable feature is that the pattern of alternation during

-32-

reperfusion was bi-directional, with T-waves occurring alternately above and below the isoelectric line (Figure 10).

The time course of onset and offset of T-wave alternans during the occlusion-release sequence coincides with the spontaneous appearance of
5   malignant tachyarrhythmias including ventricular fibrillation. Figure 12 shows a correlation between the occurrence of spontaneous ventricular fibrillation and T-wave alternans in ten dogs. Dogs which fibrillated exhibited a rapid rise in alternans within the first three or four minutes of occlusion and this change was significantly more marked than that observed in animals which survived
10   the entire occlusion-release sequence (*=p<0.001. Values are means ± S.E.M.). The results were analyzed using a one-way ANOVA with Scheffé correction for multiple comparisons. In both groups, the control values did not differ significantly from the normal distribution by the Kolmogorov-Smirnov test.

15   It is noteworthy that alternans is marked, though short lasting, during reperfusion. This transient period of heightened vulnerability to fibrillation is thought to be due to liberation of washout products of cellular ischemia. The differing mechanisms responsible for vulnerability during occlusion and reperfusion may account for the contrasting alternation pattern in T-wave
20   morphology.

The studies demonstrate that the sympathetic nervous system exerts a prominent effect on T-wave alternans, a finding which is consistent with its established arrhythmogenic influence. During coronary artery occlusion, stellectomy (Figure 11(b)) reduced alternans during the early phase of
25   occlusion [from 15.8 ± 6.6 at 4 minutes during control to 4.7 ± 1.0 mV x ms (means ± S.E.M., p<0.05)], coinciding with the time when neural activity is high in intact animals. However, later in the occlusion, extra-adrenergic factors may play a role.

Sympathetic neural influences during the reperfusion phase also appear
30   to be tracked reliably by the present techniques. It was observed that stellate ganglion ablation increased T-wave alternans during reperfusion [from 19.8 ± 3.0 to 29.8 ± 3.3 mV x ms (p<0.02)]. This concurs with a previous

-33-

study indicating that stellectomy enhances reperfusion-induced vulnerability to fibrillation. Stellate ganglion stimulation restored the magnitude of alternans to a value which was not statistically different from pre-denervation levels.

The link between alternans and vulnerability is underscored by the
5   finding that alternans coincides with the established timing of the vulnerable period in the cardiac cycle. Superimposition of successive beats indicates that alternation is restricted to the first half of the T-wave (Figures 8(b)-10(b)). This relationship remained constant in all animals studied under the changing conditions of sympathetic nervous system stimulation or denervation.

10   ANIMAL STUDY FOR HEART RATE VARIABILITY ANALYSIS

An additional animal study conducted by the inventors was performed to verify the correlation between heart rate variability and alternans. This additional study was performed substantially as set forth above. Six adult mongrel dogs were used. LAD occlusion for ten minutes was followed by
15   abrupt release. T-wave alternans appeared within three minutes of occlusion and increased to 8.97 ± 1.58 mVolts·msec by the fourth minute coinciding with maximum changes in parasympathetic (HF) activity and in the ratio of sympathetic to parasympathetic (LF:HF) activity. This is illustrated in Figure 13, where 1302 represents parasympathetic activity (HF component) and 1304
20   represents the ratio of sympathetic to parasympathetic activity (LF:HF ratio). As can be seen from inspection, sympathetic activity increases during occlusion while parasympathetic activity decreases. At reperfusion, there is no change in autonomic activity.

It is important to note that these observations concur precisely with
25   previous studies in which nerve activity to the heart was measured using recording electrodes and vulnerability to ventricular fibrillation was assessed by programmed cardiac electrical stimulation. In these experiments, it was shown that a major increase in sympathetic activity corresponded to increased susceptibility to ventricular fibrillation. See F. Lombardi, R.L. Verrier, B.
30   Lown, "Relationship between Sympathetic Neural Activity, Coronary Dynamics, and Vulnerability to Ventricular Fibrillation During Myocardial

-34-

Ischemia and Reperfusion," *American Heart Journal*, Vol. 105, 1983, pp. 958-965. A major advantage of the method of the invention is that information derived in such previous invasive studies can be obtained completely from the body surface ECG by combining heart rate variability and
5   T-wave alternans measurements.

CLINICAL APPLICABILITY

An ECG suitable for the analysis of heart rate variability is easily measured using standard surface electrode configurations. However, alternans are more difficult to sense. As discussed above, the inventors have discovered
10   that positioning the ECG sensing electrode into the apex of the left ventricle produces an optimal ECG signal for sensing alternans. This intracavitary electrode placement, however, requires invasive and hazardous procedures such that its clinical, diagnostic applicability is limited. What is needed is a method for sensing T-wave alternans non-invasively on the surface of the
15   body.

Before discussing sensing of the electrical activity of the heart, it is helpful to understand a few basic principles. The electrical signals that are sensed as an ECG include electrical currents that flow through the body as a result of depolarization and repolarization of the myocardial cells. This
20   electrical activity may be sensed as a voltage between areas of the body (e.g., between the chest proximate the heart and an arm or leg).

Theoretically, the voltage "V" at a position (x_p, y_p, z_p) due to a charge "q" at (x_i, y_j, z_k) is given by the following equation:

$$V = \frac{q}{4\pi\epsilon\sqrt{(x_p-x_i)^2+(y_p-y_j)^2+(z_p-z_k)^2}} - V_{ref} \qquad \text{Eq. (22)}$$

where: ϵ = permitivity constant

It is assumed that V_{ref} is zero for a unipolar electrode, as discussed below. If
25   the heart is modelled as a collection of charges then the equation directly

-35-

below will approximate the voltage V_{norm} sensed by an electrode located at a point (x_p, y_p, z_p).

Eq. (23)

$$V_{norm} = \sum_i \sum_j \sum_k \frac{q}{4\pi\epsilon\sqrt{(x_p - x_i)^2 + (y_p - y_j)^2 + (z_p - z_k)^2}}$$

Under stable repolarization/depolarization, the charges of the heart will repeat almost identically to create a stable ECG signal. That is, the charge

5   distribution occurring x msec after the R-wave of one cardiac cycle will be nearly identical to the charge distribution occurring x msec after the R-wave of the next cardiac cycle.

When alternans is present, however, the charge distribution will be modulated such that the charge distribution occurring x msec after the R-wave

10 of successive cardiac cycles can be modeled as a static charge distribution plus a time varying distribution representing the source of the alternans. This time varying charge distribution resulting from alternans may be represented by:

$$q_{alternans} = q \cos(2\pi f_{ALT} t)$$
$$\text{where:} \quad q = \text{the magnitude of the alternating charge}$$
$$f_{ALT} = \text{alternation frequency (Hz)} \qquad \text{Eq. (24)}$$
$$t = 0, 1, 2, \ldots \text{number of beats}$$

Locating the alternans charge at $(0,0,0)$ produces an oscillating voltage at (x_p, y_p, z_p) as follows:

$$V_{alternans} = \frac{q \cos(2\pi f_0 t)}{4\pi\epsilon\sqrt{x_p^2 + y_p^2 + z_p^2}}$$

$$\text{where:} \quad V_{alternans} = \text{the magnitude of the alternans voltage}$$
$$\text{measured at a point } (x_p, y_p, z_p)$$

Eq. (25)

-36-

This results in a total voltage at point (x_p, y_p, z_p) of:

$$V_{total} = V_{norm} + V_{alternans} \qquad \text{Eq. (26)}$$

V_{total} consists of an alternating component plus a constant component. To maximize the amount of alternating component detected, (x_p, y_p, z_p) must approach $(0,0,0)$. That is, the detecting electrode must be located as close as

5 possible to the portion of the heart that is generating the alternation signal.

For sensing a normal ECG, limb leads, such as lead II (left leg with respect to right arm) can be used. Limb leads, however, are incapable of detecting the small amplitudes of alternans. Interestingly, the inventors have discovered that alternans is a regional phenomenon that can be reliably

10 detected via the precordial ECG leads.

By regional, it is meant that the alternans emanate from the injured or ischemic portion of the heart. For example, it was found that the alternation signal is strongest in the left ventricle (LV) intracavitary ECG during a left anterior descending (LAD) coronary artery occlusion. In fact, it was noted

15 that alternation is twelve times greater as recorded from a LV intracavitary catheter as compared with a right ventricle (RV) intracavitary catheter. Corresponding to this discovery, the inventors have found that alternans could be detected in the precordial surface ECG leads corresponding to the injured portion of the heart. Note that the terms "lead" and "electrode" are used

20 interchangeably herein.

The precordial or chest leads are unipolar electrodes which sense the ECG signal at the surface of the body. A unipolar electrode senses a positive electrical current with respect to a neutral lead. The neutral lead is an average of the voltage on the three standard limb leads: left leg, left arm, and right

25 arm. Ideally, the voltage on the neutral lead is zero.

The location of the precordial leads on the body surface is shown in Figures 14(a)-(c). The precordial leads include leads V_1 through V_9 for the left side of the body and leads V_{1R} through V_{9R} for the right side of the body.

-37-

Note that lead V_1 is the same as lead V_{2R} and that lead V_2 is the same as lead V_{1R}.

The present invention is concerned primarily with precordial leads V_1 through V_6 because they are closest to the heart and, therefore, yield the

5   strongest ECG signals. Figure 15 is a cross-sectional view of the human chest area 1502 taken along a horizontal axis 1402 shown in Figures 14(a) and 14(b). Figure 15 illustrates the position of the heart 1504 in relation to front chest wall 1506. The relative positions of precordial leads V_1 through V_6 and the corresponding normal ECG signals present at each position are also shown.

10   Note that lead V_5 resides directly over the left ventricular surface.

The inventors have discovered that leads V_5 and/or V_6 are optimal for sensing alternans which result from injury to the left ventricle (e.g., obstruction of the left anterior descending artery), and leads V_1 and/or V_2 are optimal for sensing injuries such as obstruction of the right-side coronary

15   circulation. Additional precordial leads, such as V_9, may be useful for sensing alternans resulting from remote posterior wall injury. Thus, a physician may use the complete precordial lead system to obtain precise information regarding the locus of ischemia or injury.

In order to achieve the maximum sensitivity for alternans sensing,

20   attenuation by the skin and other body tissues must be reduced. Attenuation by the relatively large impedance provided by the skin can be overcome by proper skin abrasion, electrode jelly, or the use of needle electrodes. Further reduction in attenuation can be achieved by selecting the path of least resistance to the heart. This includes placing the electrodes between the ribs

25   rather than over them.

Figures 16(a)-18(a) show continuous ECG tracings obtained simultaneously from lead II, lead V_5, and a left ventricular intracavitary lead, respectively, during LAD coronary artery occlusion in a chloralose-anesthetized dog. Figures 16(b)-18(b) show superimposition of the successive

30   beats of Figures 16(a)-18(a), respectively. Note that the superimposed waveform from lead II [Figure 16(b)] shows no consistently detectable alternans. Lead V_5 [Figure 17(b)], however, shows marked alternation in the

-38-

first half of the T-wave, corresponding to the alternation observed in the intracavitary lead [Figure 18(b)].

Simultaneous comparison of T-wave alternation from lead II, lead V_5, and a left ventricular intracavitary lead during LAD coronary artery occlusion

5   in seven dogs was performed. The results are shown graphically in Figure 19 as a comparison of alternans energy from Leads II and V_5 with reference to the LV intracavitary lead. Exact correlation with the intracavitary lead will produce a line with a 45° angle. The significant linear relationship ($r^2 = 0.86$) between signals detected in V_5 and the LV intracavitary lead indicated

10 that the precordial lead can be used as a surrogate, obviating the need to place a catheter in the heart. The slope in V_5 (0.17 ± 0.05) was significantly greater than in lead II (0.08 ± 0.02) ($p < 0.001$). This finding is consistent with Equation 22 with predicts a linear relationship between the detecting electrode and the source. As shown, the signal from lead V_5 is clearly larger

15 than that of lead II. The intracavitary lead provides a stronger signal than both lead II and V_5.

Under certain clinical conditions, it may be advantageous to record alternation from the right ventricle (RV) because of the nature of the cardiac pathology. For example, under conditions of right heart hypertrophy or other

20 pathology, or right coronary artery disease, the maximum expression of alternation may be detectable from a catheter positioned in the RV. Since a catheter can be positioned from the venous side of the circulation, the RV catheterization is relatively low risk and routine.

In humans, coronary angioplasty was performed in seven patients with

25 greater than 70% stenosis of the LAD coronary artery. The angioplasty induced a three minute occlusion and reperfusion. Significant increases in T-wave alternans occurred within two minutes of occlusion and within ten seconds of release/reperfusion. Alternans occurred predominantly in leads V_2, V_3 and V_4, corresponding to the sites overlying the ischemic zone. The

30 alternans level was significantly greater than that observed in leads II, V_1, V_5 and V_6 and in the Frank leads (see E. Frank, "An Accurate, Clinically Practical System for Spatial Vectorcardiography," *Circulation*, Vol. 13, 1956,

-39-

pp. 737-749). Alternation invariably occurred in the first half of the T-wave as predicted above.

Figure 20 is a surface plot display obtained by the method of complex demodulation (as set forth above) of the T-wave of the V_4 precordial lead
5 during spontaneous heart rhythm in a representative patient during angioplasty. As can be seen, within two minutes of occlusion there was a significant increase in T-wave alternans which persisted throughout the occlusion. A marked surge in alternans upon reperfusion lasted less than one minute.

Figure 21 shows the level of T-wave alternans as a function of
10 recording site in seven patients at three minutes of angioplasty-induced occlusion and upon balloon deflation. Alternans detected during occlusion in leads V_2, V_3 and V_4 (the sites overlying the ischemic zone) was significantly greater than in leads II, V_1, V_5 and V_6. During reperfusion, alternans levels in leads V_1-V_4 were significantly greater than in leads II, V_5 and V_6.

15 CONCLUSION

The ability to sense alternans non-invasively from a surface ECG via the precordial leads and to track the alternans dynamically yields a major advance in the quest for predicting SCD. Couple this with an analysis of heart rate variability to determine the relative influence of the sympathetic and
20 parasympathetic nervous systems, and a diagnostic tool of unprecedented value in the field of cardiology results.

The inventors contemplate producing several indices for the analysis of the alternans and heart rate variability data. These include a T-wave alternans index, a heart rate variability index, and a cross-correlation index.
25 The T-wave alternans index (expressed in mV·msec) may be normalized for age, gender, medical history, heart size, heart rate, etcetera. Tables of normal data for the alternans index could be established during exercise or behavioral stress tests. Monitored values of alternans could then be compared to this standard index to yield diagnostic information on cardiac health. This includes
30 detecting and locating ischemic or injured portions of the heart. Because of the regional nature of alternans, comparison of the alternans from each

-40-

precordial lead with a corresponding standard index value for that lead would allow an ischemic or injured site to be located without the need for invasive procedures.

The alternans index may be developed along the lines of arterial blood
5   pressure indexes, for example, where pressure values in excess of 140mmHg/90mmHg are deemed to be in the range where treatment is indicated.

The heart rate variability index may be expressed as an HF amplitude (in milliseconds) and a LF/HF ratio. Normative data may be established for
10   both endpoints. It will be important to establish when sympathetic activity is excessively high and/or when parasympathetic activity is low.

The cross-correlation index recognizes that a combination of high degree of alternans and low heart rate variability indicates a condition is which the heart is particularly prone to ventricular fibrillation. This is based on the
15   fact that lowered heart rate variability indicates high sympathetic and low parasympathetic activity. It is anticipated that a mathematical function (e.g., a product of the alternans and heart rate variability indices, a power function, etcetera) will be developed to produce the cross-correlation index from the alternans index and the heart rate variability index. Empirical data will be
20   required to establish the precise quantitative relationship between the two.

It is contemplated that the invention will have great utility in the development of drugs, as their effects on autonomic activity and on the heart itself can be closely monitored.

It is further contemplated that the heart monitoring unit could be
25   miniaturized and incorporated into an implantable cardioverter/defibrillator unit to sense alternans and heart rate variability, and then deliver drugs or electricity to prevent or abort life-threatening rhythms or to revert cardiac arrest.

Although the invention has been described and illustrated with a certain
30   degree of particularity, it is understood that those skilled in the art will recognize a variety of applications and appropriate modifications within the spirit of the invention and the scope of the claims.

-41-

CLAIMS

1   1.   A method of tracking and diagnosing cardiac vulnerability
2   comprising the steps of:
3   sensing an ECG signal from a heart, said ECG signal having a plurality
4   of R-R intervals, each R-R interval including an R-wave and a T-wave;
5   analyzing said T-waves to estimate an amplitude of beat-to-beat
6   alternation, said amplitude of beat-to-beat alternation representing cardiac
7   electrical instability;
8   analyzing said R-R intervals to estimate a magnitude of a high
9   frequency component of heart rate variability and to estimate a magnitude of
10 a low frequency component of heart rate variability, said magnitude of said
11 high frequency component indicating parasympathetic neural influence on the
12 heart, said low frequency component indicating combined sympathetic and
13 parasympathetic neural influence on the heart; and
14   analyzing said amplitude of beat-to-beat alternation, said magnitude of
15 said high frequency component of heart rate variability, and said magnitude
16 of said low frequency component of heart rate variability to diagnose said
17 cardiac electrical instability.

1   2.   The method of claim 1, wherein said step of sensing an ECG
2   signal comprises the following steps:
3   placing a precordial ECG lead on the surface of a subject's body
4   proximate to the subject's heart to sense said ECG signal;
5   amplifying said ECG signal;
6   low-pass filtering said ECG signal; and
7   sampling said ECG signal.

-42-

1   3.   The method of claim 2. wherein said step of analyzing said T-
2   waves comprises the following steps:
3   predicting the location in said ECG signal of the T-wave in each R-R
4   interval;
5   partitioning each T-wave in said ECG signal into a plurality of time
6   divisions;
7   summing the samples in each of said time divisions of said ECG signal;
8   forming a time series for each of said time divisions, each time series
9   including corresponding sums from corresponding time divisions from
10   successive ones of said T-waves; and
11   performing dynamic estimation on each said time series to estimate the
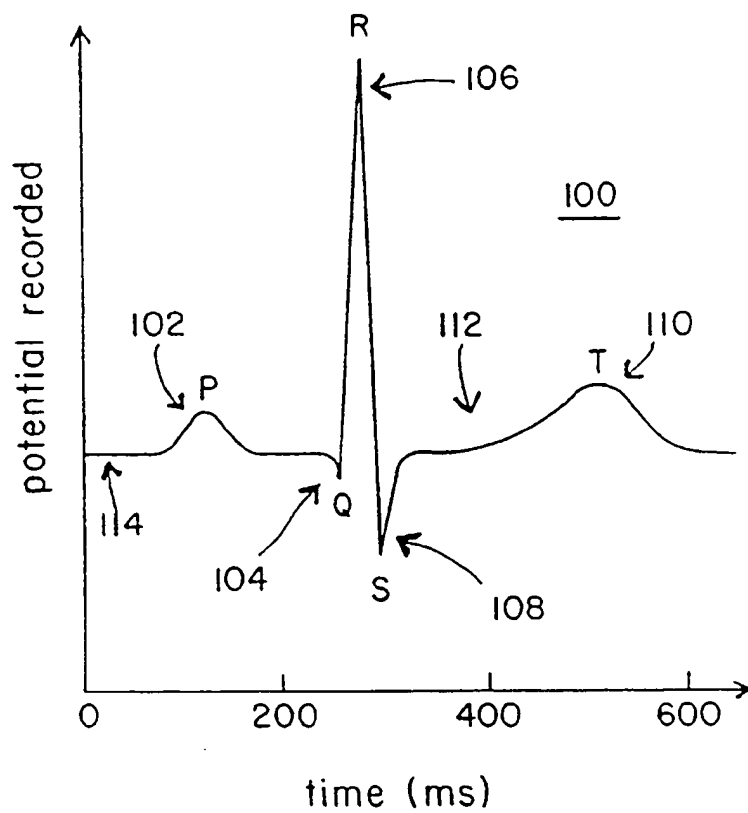12   amplitude of beat-to-beat alternation for each said time division.

1   4.   The method of claim 2, wherein said step of analyzing said R-R
2   intervals comprises the following steps:
3   locating the peak amplitude in each R-R interval to find the apex of
4   each R-wave;
5   computing the time between successive R-waves to determine a
6   magnitude of each said R-R interval;
7   forming a time series with said magnitudes of said R-R intervals;
8   .   performing dynamic estimation on said time series to estimate said
9   magnitude of said high frequency component of heart rate variability and to
10   estimate said magnitude of said low frequency component of heart rate
11   variability; and
12   forming a ratio of said magnitudes of said low frequency and said high
13   frequency components of heart rate variability, said ratio indicating
14   sympathetic activity.

1   5.   The method of claim 3, wherein said step of performing
2   dynamic estimation includes performing complex demodulation on each said
3   time series.

-43-

1   6.   The method of claim 4, wherein said step of performing

2   dynamic estimation includes performing complex demodulation on said time

3   series.

1   7.   The method of any of claims 3-6, further comprising the step

2   of comparing each R-R interval with a standard criteria to eliminate premature

3   beats.

1   8.   The method of claim 7, further comprising the step of

2   detrending each said time series prior to performing dynamic estimation in

3   order to eliminate the effects of drift and DC bias.

1   9.   A method of tracking and diagnosing cardiac vulnerability

2   comprising the steps of:

3   sensing an ECG signal from a heart, said ECG signal including a

4   plurality of R-R intervals and a plurality of T-waves;

5   analyzing said T-waves to estimate an amplitude of beat-to-beat

6   alternation, said amplitude of beat-to-beat alternation representing cardiac

7   electrical stability;

8   analyzing said R-R intervals to characterize heart rate variability;

9   estimating the magnitude of a high frequency component of heart rate

10   variability, said magnitude of said high frequency component indicating

11   parasympathetic activity;

12   estimating the magnitude of a low frequency component of heart rate

13   variability;

14   forming a ratio of said low frequency and said high frequency

15   components of heart rate variability, said ratio indicating sympathetic activity;

16   and

17   analyzing said amplitude of beat-to-beat alternation, said magnitude of

18   said low frequency component of heart rate variability, and said ratio of said

19   low frequency and said high frequency components of heart rate variability to

20   diagnose said cardiac electrical stability.

-44-

1   10.   The method of claim 9, wherein said step of sensing an ECG

2   signal comprises the following steps:

3   placing a precordial ECG lead on the surface of a subject's body

4   proximate to the subject's heart to sense said ECG signal;

5   amplifying said ECG signal;

6   low-pass filtering said ECG signal; and

7   sampling said ECG signal.

1   11.   The method of claim 10, wherein said step of analyzing said T-

2   waves comprises the following steps:

3   predicting the location in said ECG signal of the T-wave in each R-R

4   interval;

5   partitioning each T-wave in said ECG signal into a plurality of time

6   divisions;

7   summing the samples in each of said time divisions of said ECG signal;

8   forming a time series for each of said time divisions, each time series

9   including corresponding sums from corresponding time divisions from

10   successive ones of said T-waves; and

11   performing dynamic estimation on each said time series to estimate the

12   amplitude of beat-to-beat alternation for each said time division.

1   12.   The method of claim 10, wherein said step of analyzing said R-

2   R intervals comprises the following steps:

3   locating the peak amplitude in each R-R interval to find the apex of

4   each R-wave;

5   computing the time between successive R-waves to determine a

6   magnitude of each said R-R interval; and

7   forming a time series with said magnitudes of said R-R intervals.

1   13.   The method of claim 12, wherein said steps of estimating the

2   magnitude of low and high frequency components of heart rate variability are

3   performed using complex demodulation.

1   14.   The method of claim 11, wherein said step of performing

2   dynamic estimation includes performing complex demodulation on each said

3   time series.

1   15.   An apparatus for dynamically tracking and diagnosing cardiac

2   vulnerability by simultaneously analyzing T-wave alternation and heart rate

3   variability in an ECG having a plurality of R-R intervals, said apparatus

4   comprising:

5   means for sampling the ECG;

6   means for predicting the location in the ECG signal of the T-wave in

7   each R-R interval;

8   means for analyzing said T-waves to determine an amplitude of beat-to-

9   beat alternation;

10   means for computing the magnitude of each R-R interval to determine

11   a heart rate;

12   means for analyzing said heart rate to determine a variability therein,

13   for computing a magnitude of a high frequency component of said variability

14   indicative of parasympathetic neural influence on a heart and a magnitude of

15   a low frequency component of said variability indicative of combined

16   sympathetic and parasympathetic neural influence on said heart, and for

17   computing a ratio of said low frequency component to said high frequency

18   component, said ratio indicating sympathetic neural influence on said heart;

19   and

20   means for presenting said amplitude of beat-to-beat alternation, said

21   high frequency component of said variability and said ratio to a user.

FIG. IA

FIG. IB

FIG. 2A

FIG. 2B

```
┌──────────────────────────────┐
│  TERFENADINE (SELDANE)       │
│     + ANTIBIOTIC             │──── 202
└──────────────────────────────┘
               │
               ▼
        ┌ ─ ─ ─ ─ ─ ─ ─ ┐
        │               │
        └ ─ ─ ─ ─ ─ ─ ─ ┘
               │
               ▼
┌──────────────────────────────┐
│     T-WAVE ALTERNANS         │──── 206
└──────────────────────────────┘
               │
               ▼
┌──────────────────────────────┐
│     SUDDEN CARDIAC           │
│        DEATH                 │──── 208
└──────────────────────────────┘
```

FIG. 2C

HIGH DOSE OF
DIGITALIS ∼202

DECREASED
HRV ∼204

T-WAVE ALTERNANS ∼206

SUDDEN CARDIAC
DEATH ∼208

FIG. 3

PATIENT

SENSE ECG SIGNAL — 302

HIGH-PASS FILTER
ECG SIGNAL — 304

AMPLIFY — 306

LOW-PASS FILTER — 308

DIGITIZE — 310

STORE DIGITIZED
ECG SIGNAL — 312

DYNAMICALLY PROCESS
DIGITIZED ECG SIGNAL — 314

FIG. 4

DIGITIZED ECG SIGNAL

FIND PEAK AMPLITUDE FOR EACH R-R
INTERVAL TO LOCATE APEX OF R-WAVE — 404

REMOVE PREMATURE BEATS — 406

IDENTIFY T-WAVE DATA
FOR EACH R-R INTERVAL — 408

PARTITION EACH T-WAVE INTO (B) TIME DIVISIONS — 410

COMPUTE THE AREA OF EACH DIVISION — 412

FORM A TIME SERIES FOR EACH TIME DIVISION
USING CORRESPONDING TIME DIVISIONS FROM
(N) SUCCESSIVE T-WAVES — 414

DETREND EACH TIME SERIES TO REMOVE
DRIFT AND DC BIAS — 416

ESTIMATE ALTERNATION AMPLITUDE
FOR EACH TIME SERIES — 418

Digitized ECG signal

Find peak amplitude for each R-R
interval to locate apex of R-waves ── 504

Compute R-R intervals ── 506

Remove premature beats ── 508

Form a time series of R-R interval
data ── 510

Form a new sequence (R$_t$) along the same time
line, whose points are 100 msec apart and whose
values are the R-R interval present at that time ── 512

High pass filter the sequence (R$_t$)
to remove any low frequency trends ── 514

516 ─┐

Estimate the amplitude of the
Low frequency component of HRV

Low pass filter ── 518

520 ─┐
Divide low frequency component by the high
frequency component on a point by point
basis

Sympathetic Activity

522 ─┐
Estimate the amplitude of the
High frequency component of HRV

524 ─── Low pass filter

Parasympathetic Activity

FIG. 5

FIG. 6A

PATIENT

└─ 601

| ECG DETECTOR AND PRE-PROCESSOR | ─ 602 |

600
↙

| ECG PROCESSING SYSTEM | ─604 |

FIG. 6B

602
↘

PATIENT

└─ 601

| HIGH-PASS FILTER | ─ 6022 |

| PRE-AMPLIFIER | ─ 6024 |

| LOW-PASS FILTER | ─ 6026 |

TO ECG
PROCESSING SYSTEM 604

FIG. 6C

604

ECG SIGNAL

DATA STORAGE — 6046

6050

ANALOG-TO-DIGITAL CONVERTER

6040

OPERATING SYSTEM

6045

6041

6043
RAM

6042
CPU

6044
I/O INTERFACE

6047

PRINTER — 6049

6048

Heart Monitoring Unit

600

Patient

718

VGA Color Monitor

Menu Driven Program
  1. Data Acquisition
     a. Set Sampling Rate
     b. Select ECG Channels
     c. Set Input Gain
     d. Name Data File
     e. Start A/D Conversion
  2. Data Analysis
     a. Trend Removal
     b. Removal of Arrhythmias
     c. Dynamic T-wave Analysis
     d. Dynamic HR Variability Analysis
  3. Display
     a. ECG Waveforms
     b. T-wave Area Sequencing
     c. Detrended T-wave Area
     d. Dynamic T-wave Result
     e. Dynamic HR Variability Result

704

16 Channel
0.01 Hz. ECG
Filters

706

16 Channel
Op-Amp
Preamplifiers

708

16 Channel
50 Hz.
Antialiasing
Filter

Personal Computer

710

120 MByte Hard Drive
3 1/2" Floppy Drive

16 Channel A/D Converter
w/Programmable Gain

712

FIG. 7

716

Rewritable Optical
Drive for
Archiving Data

714

Printer for
Hard Copy
Output

FIG. 8A Control — Continuous

FIG. 8B — Superimposed

10mV

FIG. 9A Occlusion

FIG. 9B

FIG. IOA Reperfusion

FIG. IOB

400msec

400msec

FIG. 11A

FIG. 11B

Sympathetic Stimulation

FIG. IIC

FIG. 12

FIG. 13

FIG. 14A

MIDCLAVICULAR LINE

ANTERIOR AXILLARY LINE

MIDAXILLARY LINE

1402

HORIZONTAL
PLANE OF V_{4-6}

V_1 V_2 V_3 V_5 V_6
V_4
$(V_{2R})(V_{1R})$

V_{6R} V_{4R}
V_{5R} V_{3R}

FIG. 14B

V_7 V_8 V_9 V_{9R} V_{7R}
V_{8R}

V_1 V_2
V_3
V_4 V_5 V_6

FIG. 14C

SUBSTITUTE SHEET

FIG. 15

During Coronary Artery Occlusion in the Dog

LEAD II (CONTINUOUS)

FIG. 16A

LEAD II (SUPERIMPOSED)

FIG. 16B

PRECORDIAL (V5) (CONTINUOUS)
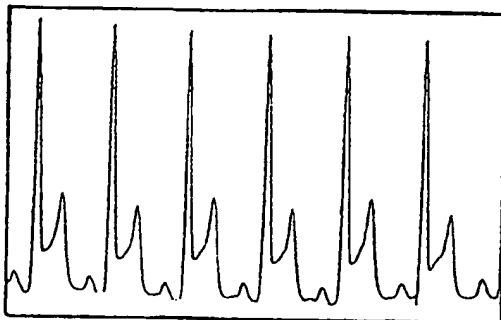
FIG. 17A

PRECORDIAL (V5) (SUPERIMPOSED)
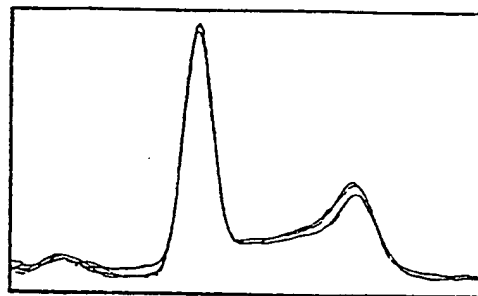
FIG. 17B

LEFT VENTRICULAR
INTRACAVITARY (CONTINUOUS)
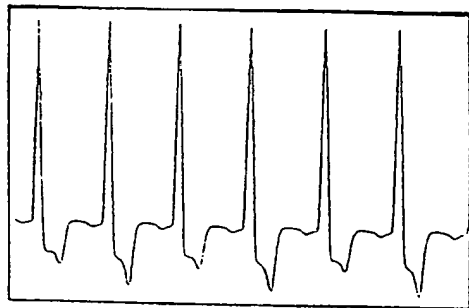
FIG. 18A

LEFT VENTRICULAR
INTRACAVITARY (SUPERIMPOSED)
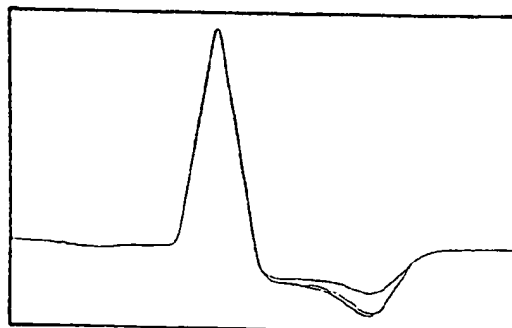
FIG. 18B

SUBSTITUTE SHEET
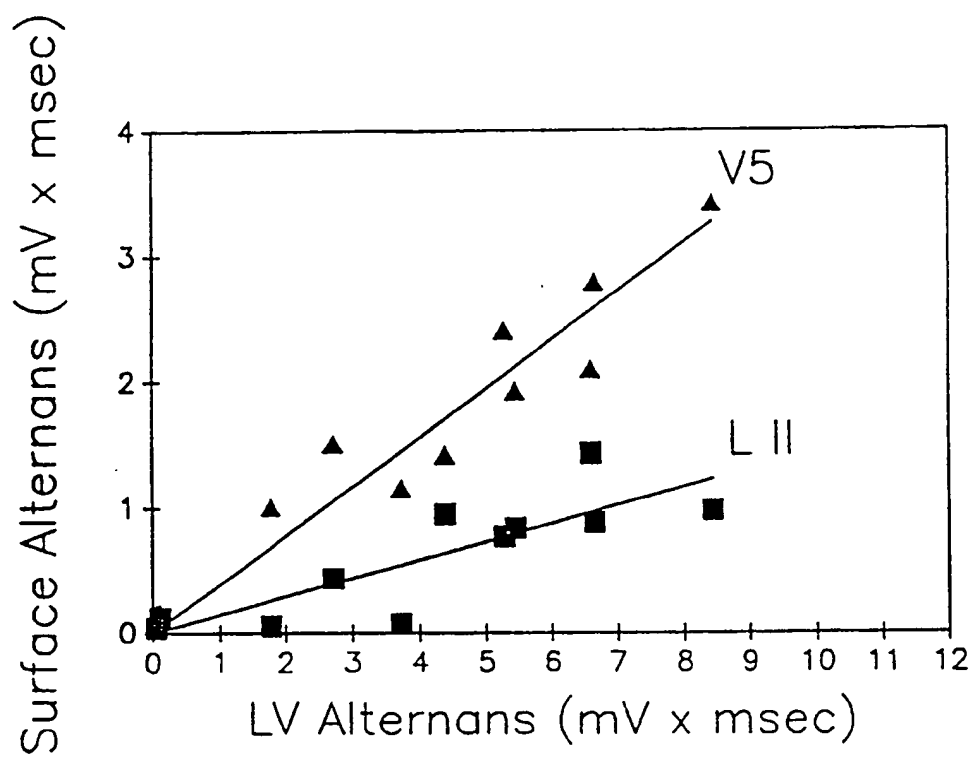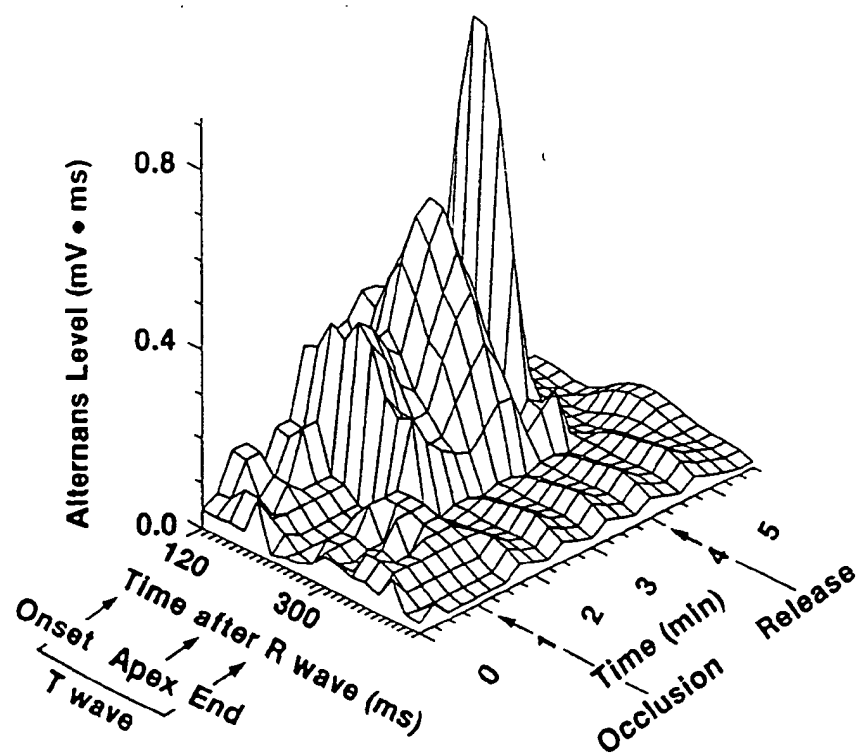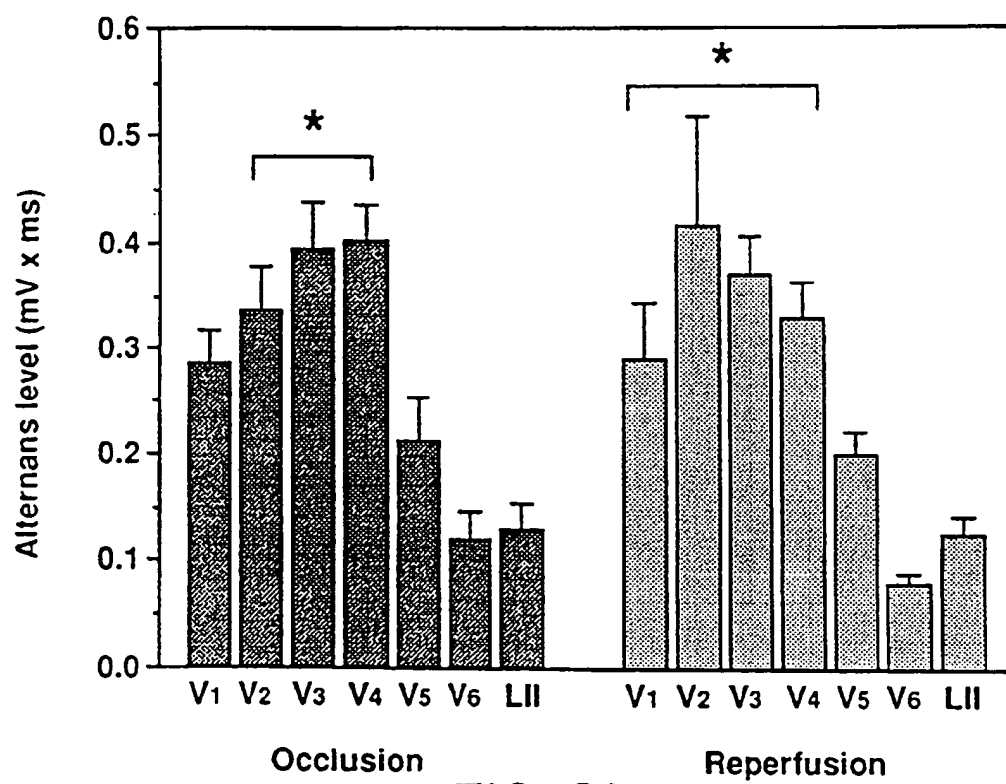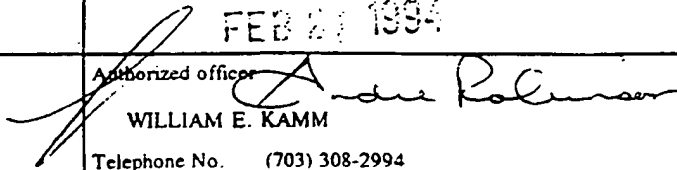
FIG. 19

FIG. 20

FIG. 21

INTERNATIONAL SEARCH REPORT

A. CLASSIFICATION OF SUBJECT MATTER

IPC(5)   :A61B 5/0452
US CL   :128/704

According to International Patent Classification (IPC) or to both national classification and IPC

B. FIELDS SEARCHED

Minimum documentation searched (classification system followed by classification symbols)

U.S. :   128/72, 703-705

Documentation searched other than minimum documentation to the extent that such documents are included in the fields searched

None

Electronic data base consulted during the international search (name of data base and, where practicable, search terms used)

None

C. DOCUMENTS CONSIDERED TO BE RELEVANT

Category*	Citation of document, with indication, where appropriate, of the relevant passages	Relevant to claim No.
A	US, A, 5,020,540 (Chamoun) 04 June 1991	
A	US, A, 5,109,862 (Kelen et al.) 05 May 1992	
A	US, A, 5,092,341 (Kelen) 03 March 1992.	
A	US, A, 4,583,553, (Shah et al.) 22 April 1986	
A	US, A, 4,492,235 (Sitrick) 08 January 1985	
A	US, A, 4,796,638 (Sasaki) 10 January 1989	

[X] Further documents are listed in the continuation of Box C.   [ ]   See patent family annex.

* Special categories of cited documents:	"T" later document published after the international filing date or priority date and not in conflict with the application but cited to understand the principle or theory underlying the invention
"A" document defining the general state of the art which is not considered to be part of particular relevance	
"E" earlier document published on or after the international filing date	"X" document of particular relevance; the claimed invention cannot be considered novel or cannot be considered to involve an inventive step when the document is taken alone
"L" document which may throw doubts on priority claim(s) or which is cited to establish the publication date of another citation or other special reason (as specified)	"Y" document of particular relevance; the claimed invention cannot be considered to involve an inventive step when the document is combined with one or more other such documents, such combination being obvious to a person skilled in the art
"O" document referring to an oral disclosure, use, exhibition or other means	
"P" document published prior to the international filing date but later than the priority date claimed	"&" document member of the same patent family

Date of the actual completion of the international search	Date of mailing of the international search report
27 December 1993	FEB ?? 1994
Name and mailing address of the ISA/US
Commissioner of Patents and Trademarks
Box PCT
Washington. D.C. 20231	Authorized officer
WILLIAM E. KAMM
Facsimile No. NOT APPLICABLE	Telephone No. (703) 308-2994

Form PCT/ISA/210 (second sheet)(July 1992)*

INTERNATIONAL SEARCH REPORT

C (Continuation). DOCUMENTS CONSIDERED TO BE RELEVANT

Category*	Citation of document, with indication, where appropriate, of the relevant passages	Relevant to claim No.
A	US, A, 4,680,708 (Ambos et al.) 14 July 1987	